Quantum and temperature effects on Davydov soliton dynamics. III. Interchain coupling

1993 J. Phys.: Condens. Matter 5 823

(http://iopscience.iop.org/0953-8984/5/7/009)

J. Phys.: Condens. Matter 5 (1993) 823–840. Printed in the UK

Quantum and temperature effects on Davydov soliton dynamics: III. Interchain coupling†

Wolfgang Förner

Department of Theoretical Chemistry, and Laboratory of the National Foundation of Cancer Research, Friedrich-Alexander University Erlangen-Nürnberg, Egerlandstrasse 3, W-8520 Erlangen, Federal Republic of Germany

Received 24 July 1992

Abstract. We show numerically that Scott's suggestion to use revised parameter values in order to simulate interchain coupling effects on Davydov soliton dynamics with one-chain simulations is correct also for excitations within the $|D_2\rangle$ *ansatz* state, for which his analytical derivation does not hold. However, in the case of the $|D_1\rangle$ state we find that the equations of motion for the symmetric mode reduce exactly to the equations for one chain without any renormalization of parameters. Further, we present numerical simulations for three coupled chains including temperature within different *ansatz* states and for one chain using Scott's revised parameters. We found that Davydov solitons should exist in three-chain systems at physiological temperature for reasonable parameter values.

1. Introduction

For the mechanism of energy transport through proteins Davydov [1,2] suggested that the energy of $\simeq 0.4$ eV released by hydrolysis of adenosine triphosphate (ATP) could be transported in quanta of the amide-I (mainly C=O stretch) vibration ($\simeq 0.2$ eV). The CO groups participate in hydrogen bonds, which form chains parallel to the axis of α-helical proteins. Thus the amide-I vibration interacts with the acoustic phonons in these chains. The excitation of an amide-I oscillator causes a distortion in the lattice, which in turn stabilizes the amide-I excitation [1,2]. It was found that for certain regions of the parameter space of the model this effect can prevent the excitation from dispersion via the dipole–dipole coupling between neighbouring CO groups in the lattice. The region in which the vibrational energy is localized can travel as a soliton along the chain. In his original theory Davydov [1] used an *ansatz* for the wavefunction ($|D_2\rangle$) that treats the lattice classically. At zero temperature it has been confirmed that Davydov solitons exist for parameter values appropriate for proteins [3]. Also their stability against disorder along the chain was studied [4]. The investigation of temperature led to controversial results [5–14].

Brown *et al* [15] have shown that the $|D_2\rangle$ state *ansatz* does not reproduce the dynamics of the exactly solvable small-polaron limit (dipole–dipole coupling neglected). Davydov [2] introduced a more sophisticated *ansatz* state ($|D_1\rangle$, see also

† Dedicated to Professor Alwyn C Scott on the occasion of his 60th birthday.

0953-8984/93/070823+18$07.50

[16]), which allows for quantum effects in the lattice. However, he used the energy expectation value for $|D_1\rangle$ as classical Hamiltonian function to derive equations of motion [2]. It was shown that with these equations $|D_1\rangle$ does not reproduce the small-polaron limit [15] either. Mechtly and Shaw [17] and Skrinjar *et al* [18] could derive new equations of motions for $|D_1\rangle$ with the help of quantum-mechanical methods. These equations of motion reproduce the small-polaron limit. However, in the general case also this *ansatz* state is still approximate. In [17] as well as in our work [19] it is shown that at $T = 0$ K the window for travelling solitons in the $|D_1\rangle$ state occurs in regions of the parameter space that cannot be applied to proteins (soliton formation threshold $X > 150$ pN).

In the first paper of this series [20] we also used the Langrangian method described in [18] to obtain correct equations of motion for the $|D_1\rangle$ *ansatz* state from the thermally averaged Hamiltonian derived in [2, 16]. In this investigation [20, 21], as well as in our previous studies within the $|D_2\rangle$ state, summarized in [21], we found that Davydov solitons should be stable at 300 K if the spring constant of the hydrogen bonds is larger than previously assumed. There are doubts if the Davydov concept of using a thermally averaged Hamiltonian to derive equations of motion from it is in agreement with statistical mechanics. There is the possibility that it may lead to results that are even qualitatively misleading. Therefore we performed comparisons of our results obtained with the averaged Hamiltonian method with the exact quantum Monte Carlo results of Wang *et al* [22]. We found (see the second paper of this series [23]) that, in contrast to other models for temperature effects, Davydov's *ansatz* reproduces the results given in [22] at least qualitatively. Therefore we use this *ansatz* also in this work in order to investigate temperature and interchain coupling effects. Since all our results indicate that the hydrogen-bond spring constant should be large to allow soliton formation at 300 K, we go back to the suggestion of Scott [3, 24, 25] that in one-chain simulations the spring constant should be larger by a factor of 3, in order to simulate the three coupled chains present in real protein α-helices within a one-chain model. Scott reached this conclusion from analytical considerations on a symmetric excitation mode and from dynamical simulations on three chains [3]. For an excellent review of the state of the art of work on Davydov solitons, the reader should consult Scott's recent paper [25]. In the second section of this work we briefly describe Davydov's two *ansatz* states for one chain, and in the third part we present one-chain simulations using the $|D_1\rangle$ state with revised parameters according to Scott's suggestion. In the fourth part we present simulations on three chains using different excitations (symmetric as well as asymmetric ones) within the $|D_2\rangle$ *ansatz* state and compare them with one-chain results, using different parameter values. We could confirm Scott's conclusion about parameter values also for excitations he did not consider, and for which his analytical considerations do not hold. However, within the $|D_1\rangle$ model we found that for the symmetric A mode the equations of motion for one spine and for three coupled chains are identical. Finally in the fifth part some examples of three-chain simulations including temperature are discussed, and in the sixth part the results obtained are summarized.

2. *Ansatz* states

2.1. The $|D_2\rangle$ ansatz

In this section we describe briefly the *ansatz* states of Davydov for the case of one

chain and the models we used to introduce temperature effects. The Hamiltonian is in the case of one chain [1] given by

$$\hat{H} = \sum_n [E_0 \hat{a}_n^+ \hat{a}_n - J_n(\hat{a}_n^+ \hat{a}_{n+1} + \hat{a}_{n+1}^+ \hat{a}_n) + \frac{\hat{p}_n^2}{2M_n} + \frac{W_n}{2}(\hat{q}_{n+1} - \hat{q}_n)^2 + X_n \hat{a}_n^+ \hat{a}_n (\hat{q}_{n+1} - \hat{q}_n)]. \tag{1}$$

The meaning of the operators in equation (1) as well as the explanation and values of the parameters are given in paper II of this series [23] (see also figure 1).

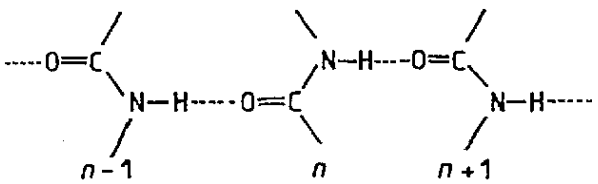

Figure 1. Schematic picture of a hydrogen-bonded channel in a protein.

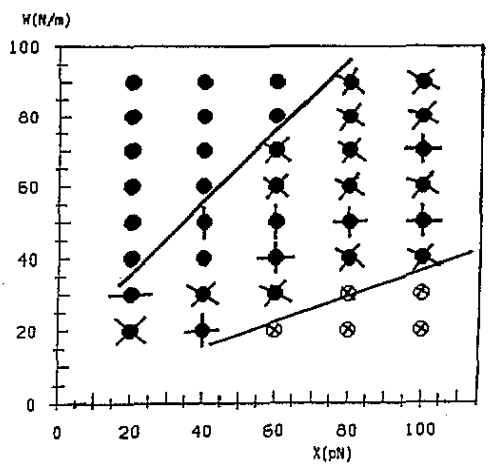

Figure 2. Survey of the (X, W) parameter space at $T = 300$ K using Davydov's temperature model and the $|D_1\rangle$ *ansatz* state for one chain together with a mass of $3M = 342m_p$ (initial excitation at site 49, time step 0.15 fs, chains of 50 units). Crossed open circles: pinned soliton. Horizontally dashed black circle: pinning or reflection after roughly 40 sites. Vertically dashed black circles: slowly dispersive solitary wave. Horizontally/vertically crossed black circles: soliton that becomes pinned after a few sites. Diagonally crossed black circles: moving soliton that becomes pinned after interaction with the shock wave and then slowly disperses. Uncrossed black circle: travelling soliton.

For the approximate solution of the time-dependent Schrödinger equation Davydov [1] introduced the displaced oscillator state *ansatz* called $|D_2\rangle$. Davydov [1, 2] formed the expectation value of the Hamiltonian (1) with $|D_2\rangle$ and used this

expectation value as classical Hamiltonian function. In this way he obtained the equations of motion. Kerr and Lomdahl [7] have shown that these equations can be obtained also by purely quantum-mechanical methods and also for states of more than one quantum [8]. The $|D_2\rangle$ state reproduces the lattice dynamics for $J = 0$ correctly, but leads to an incorrect phonon energy [15]. For the inclusion of temperature, we first solve the decoupled lattice problem ($X = 0$) [13, 14], which is simply a chain of coupled harmonic oscillators. As initial excitations we distribute an energy of Nk_BT (k_B is Boltzmann's constant) on the normal modes using Bose–Einstein statistics. Half of this energy was distributed as potential, the other half as kinetic energy. Thus the lattice displacements and momenta at a given time t_0 after equilibration can be obtained analytically and incorporated into the equations of motion via a phase transformation (see [21] for details). The time t_0 can be chosen arbitrarily. The results of soliton dynamics do not depend on the choice of t_0 as we have shown in [4].

2.2. *The $|D_1\rangle$ ansatz state*

In this section we show briefly the equations for the $|D_1\rangle$ *ansatz* state in the case of one chain [20,21]. The Hamiltonian [1,2] in second quantized form including disorder is given by

$$\hat{H} = \sum_n [(E_0 + E_n)\hat{a}_n^+ \hat{a}_n - J_n(\hat{a}_{n+1}^+ \hat{a}_n + \hat{a}_n^+ \hat{a}_{n+1})] + \sum_k \hbar\omega_k \left(\hat{b}_k^+ \hat{b}_k + \tfrac{1}{2} + \sum_n B_{nk}(\hat{b}_k + \hat{b}_k^+)\hat{a}_n^+ \hat{a}_n \right)$$

$$B_{nk} = \frac{X_n}{\omega_k} \left(\frac{1}{2\hbar\omega_k} \right)^{1/2} \left(\frac{U_{n+1,k}}{M_{n+1}^{1/2}} - \frac{U_{nk}}{M_n^{1/2}} \right). \tag{2}$$

Here $\hat{b}_k^+ (\hat{b}_k)$ are creation (annihilation) operators for acoustic phonons of wavenumber k. The translational mode has to be excluded from the summation. Note that we use again the asymmetric interaction model where only the coupling of the oscillator n to the hydrogen bond between n and $n + 1$ in which the oscillator takes part is considered. In (2) ω_k denotes the eigenfrequency of the normal mode k and $\mathbf{U}$ contains the normal mode coefficients; ω and $\mathbf{U}$ are obtained by numerical diagonalization of the matrix $\mathbf{V}$ with elements

$$V_{nm} = \{[W_n(1 - \delta_{nN}) + W_{n-1}(1 - \delta_{n1})]\delta_{nm} - W_n(1 - \delta_{nN})\delta_{m,n+1} - W_{n-1}(1 - \delta_{n1})\delta_{m,n-1}\}(M_n M_m)^{-1/2}. \tag{3}$$

The form of $\mathbf{V}$ implies that we use free chain ends and N units. Other boundary conditions like cyclic [16] or fixed chain ends [17] would require another form of $\mathbf{V}$.

The $|D_1\rangle$ *ansatz* for inclusion of temperature in Davydov's approximation for solution of the time-dependent Schrödinger equation is

$$|D_1, \nu\rangle = \sum_n a_n'(t)\hat{a}_n^+ |0\rangle_e |\beta_n, \nu\rangle. \tag{4}$$

Here $|0\rangle_e$ is the exciton vacuum, and $|\beta_n, \nu\rangle$ is a coherent phonon state. For the one-quantum oscillator states used here $\sum_n |a'_n|^2 = 1$ holds. To include temperature approximately we assume, as in [16], that a phonon distribution

$$|\nu\rangle = \prod_k \frac{1}{(\nu_k!)^{1/2}} (\hat{b}_k^+)^{\nu_k} |0\rangle_p \tag{5}$$

is present in the lattice where each normal mode is occupied by ν_k quanta. Here $|0\rangle_p$ is the phonon vacuum. We do not consider a thermal distribution of amide-I quanta since at 300 K the Boltzmann factor implies that only 3 of 10000 amide-I oscillators would be thermally excited. Thus one can neglect a possible thermalized soliton distribution in the system too, since the presence of solitons requires first of all amide-I excitation. Then

$$|\beta_n, \nu\rangle = \exp\left(\sum_k [b_{nk}(t)\hat{b}_k^+ - b_{nk}^*(t)\hat{b}_k]\right)|\nu\rangle \tag{6}$$

where the $b_{nk}(t)$ are the coherent state amplitudes. Following the derivation of Cruzeiro *et al* [16] (done for cyclic ordered chains) we obtain the thermally averaged Hamiltonian

$$H_T = \sum_n \Big((E_0 + E_n)|a'_n|^2 - J_n a_n'^* a'_{n+1} D_{n,n+1} - J_{n-1} a_n'^* a'_{n-1} D_{n,n-1} + |a'_n|^2 \sum_k \hbar\omega_k [B_{nk}(b_{nk} + b_{nk}^*) + v_k + \tfrac{1}{2} + |b_{nk}|^2] \Big) \tag{7}$$

with

$$v_k = \frac{1}{\exp(\hbar\omega_k / k_B T) - 1} \tag{8}$$

(Bose–Einstein statistics) and

$$D_{nm} = \exp\left(\sum_k [(v_k + 1) b_{nk}^* b_{mk} + v_k b_{nk} b_{mk}^* - (v_k + \tfrac{1}{2})(|b_{nk}|^2 + |b_{mk}|^2)]\right). \tag{9}$$

The equations of motion are derived with the Euler–Lagrange formalism following [18] and one obtains finally (see [20])

$$i\hbar \dot{a}_n = -\frac{i\hbar}{2} a_n \sum_k (\dot{b}_{nk} b_{nk}^* - \dot{b}_{nk}^* b_{nk}) + E_n a_n - J_n D_{n,n+1} a_{n+1} - J_{n-1} D_{n,n-1} a_{n-1} + a_n \sum_k \hbar\omega_k [B_{nk}(b_{nk} + b_{nk}^*) + |b_{nk}|^2]$$

$$a'_n(t) = a_n(t)\exp\left[-\frac{\mathrm{i}}{\hbar}\left(E_0 + \sum_k \hbar\omega_k(v_k + \tfrac{1}{2})\right)t\right] \tag{10}$$

$$\begin{aligned}\mathrm{i}\hbar\dot{b}_{nk} = {} & \hbar\omega_k(B_{nk} + b_{nk}) - J_n(b_{n+1,k} - b_{nk}) \\ & \times [(v_k + 1)D_{n,n+1}(a_{n+1}/a_n) + v_k D_{n+1,n}(a^*_{n+1}/a^*_n)] \\ & - J_{n-1}(b_{n-1,k} - b_{nk})[(v_k + 1)D_{n,n-1}(a_{n-1}/a_n) \\ & + v_k D_{n-1,n}(a^*_{n-1}/a^*_n)].\end{aligned}$$

To avoid numerical difficulties due to the denominators a_n and a^*_n we used as initial condition ($N = 50$):

$$a_n(0) = A[\delta_{n,n_0} + x_n(1 - \delta_{n,n_0})] \tag{11}$$

where A is the normalization constant, $x_n = 0.005$ as in [17] and $n_0 = 49$. One has to emphasize here that, owing to the translational invariance of the Hamiltonian for infinite or cyclic chains without disorder, all stationary states have also to be translationally invariant. However, because of the localized initial excitation we have to deal with the time evolution of non-stationary states that ideally (the $|D_1\rangle$ *ansatz* is an approximation) solve the time-dependent Schrödinger equation, although they are not eigenstates of the Hamiltonian. Owing to the localized initial excitation, also an exact solution for the time evolution of this initial state would not be translationally invariant, although in principle this exact solution could be expanded in the space of the (unknown) stationary and translationally invariant eigenstates of the Hamiltonian. The method introduced by Davydov to describe temperature effects, which we also apply in this work, was criticized by several authors as being inconsistent with statistical mechanics, since equations of motion are obtained from a thermally averaged Hamiltonian. However, as we have found previously [23], the results obtained with this model agree qualitatively with exact quantum Monte Carlo results from [22].

3. One-chain dynamics at $T = 300$ K with enlarged mass

In this section we want to follow Scott's suggestion to use revised parameters in one-chain dynamics in order to simulate three-chain dynamics with them. Since we want to survey the (X, W) parameter space, we only need to change the site mass from $114m_p$ to $342m_p$ (m_p = proton mass). However, we have to keep in mind that then in these simulations W is an effective spring constant and no longer the spring constant of an individual hydrogen bond. We used chains of 50 units and an initial excitation at one site (49) as in the calculations reported previously [20]. The temperature was 300 K using Davydov's model for temperature effects and the $|D_1\rangle$ *ansatz* state. The time step was 0.15 fs and we followed the dynamics over roughly 26 ps using a fourth-order Runge–Kutta method for the numerical solution of the equations of motion. In the case of the $|D_1\rangle$ state Scott's analytical considerations for a symmetric A-mode excitation within the $|D_2\rangle$ state, which are repeated in brief in the next section, do not hold. Thus we should not expect that also for the $|D_1\rangle$ *ansatz* the three-chain case is reproduced by one-chain dynamics if we use precisely

$3W$ and $3M$ instead of W and M. However, because a survey of the parameter space requires a large number of simulations, it would be preferable if one could work with the one-chain model, since it needs less computation time and thus longer chains can be used (50 units).

The results of our calculations are displayed in figure 2. Since the enlarged mass influences considerably the phonon frequencies, we have to expect that interactions between the soliton and sound waves in the lattice might be different from the one-chain case with small site mass. Indeed, this is the case, as the figure shows. We find many parameter values where the solitons become pinned after interaction with the sound wave reflected from the chain end. After that interaction, in most cases the solitons disperse slowly and perform a random walk around the pinning site. For $W = 80$ N m^{-1} and $X = 60$ pN the soliton is even reflected from the shock wave, but not destroyed. Therefore we marked this point in the parameter space as a point where travelling solitons exist. In general we see that the picture is very similar to that for the reduced value of the mass [20]. The region of stable solitons is again shifted to small X and rather large W values, and the boundary of this region appears to be roughly linear. However, here W has another meaning than in previous work on one chain. Thus the threshold for soliton formation of $W \simeq 40$ N m^{-1} should correspond to a spring constant for single hydrogen bonds of roughly 13 N m^{-1}, which is the usually cited value, while the also used value of 19 N m^{-1} corresponds here to $W \simeq 60$ N m^{-1}. However, the factor of 3 holds only for $|D_2\rangle$ theory, while for $|D_1\rangle$ this is not the case. Further the figure shows that for a value $X = 60$ pN W has to be larger than 70 N m^{-1} to allow travelling solitons, which corresponds to a hydrogen-bond spring constant of $\simeq 25$ N m^{-1}, which is larger than the usually used value taken from crystalline formamide. Since we know that Davydov's model for temperature effects, although criticized, reproduces exact quantum Monte Carlo (QMC) results qualitatively [23], we can expect from these results that Davydov solitons should be possible in protein helices at $T = 300$ K, again as in the $|D_2\rangle$ case, if W is in the region around 30 N m^{-1}. However, since we do not know to which value of the hydrogen spring constant a given value of W corresponds in our case, we have to find out how the exact $|D_1\rangle$ equations for three chains simplify in the case of the A mode and we also have to perform explicit three-chain simulations, which we can compare with one-chain dynamics for different values of W. This will be discussed in the next section.

But let us turn first to some explicit dynamic results. For this purpose we show in figure 3 the time evolution of the probability $|a_n(t)|^2$ to find an amide-I excitation at site n and the squared lattice displacement $D_n(t) = [q_{n+1}(t) - q_n(t)]^2$ for four of the cases summarized in figure 3. In figure 3(a) the case $W = 40$ N m^{-1} and $X = 20$ pN is shown, where an interesting phenomenon occurs: after interaction between the soliton and the sound wave in the lattice the major part of the excitation is reflected from the interaction site and travels backwards in the form of a soliton. However, from that part of the excitation which remains at the interaction site a second soliton is formed, which also travels backwards but with reduced velocity. In figure 3(b) we show the dynamics for $W = 40$ N m^{-1} again and for $X = 40$ pN. We see that in this case a soliton travels through the chain, broadens after interaction with the sound wave, and close to the end of the simulation time two solitons are formed which travel into opposite directions. In the case of $W = 60$ N m^{-1} and $X = 20$ pN (figure 3(c)) we observe a soliton that survives interaction with the shock wave, as well as reflection at the chain end. For $X = 40$ pN and the same W

(figure 3(*d*)) the soliton also travels through the chain, but during interaction with the sound wave its amplitude becomes smaller.

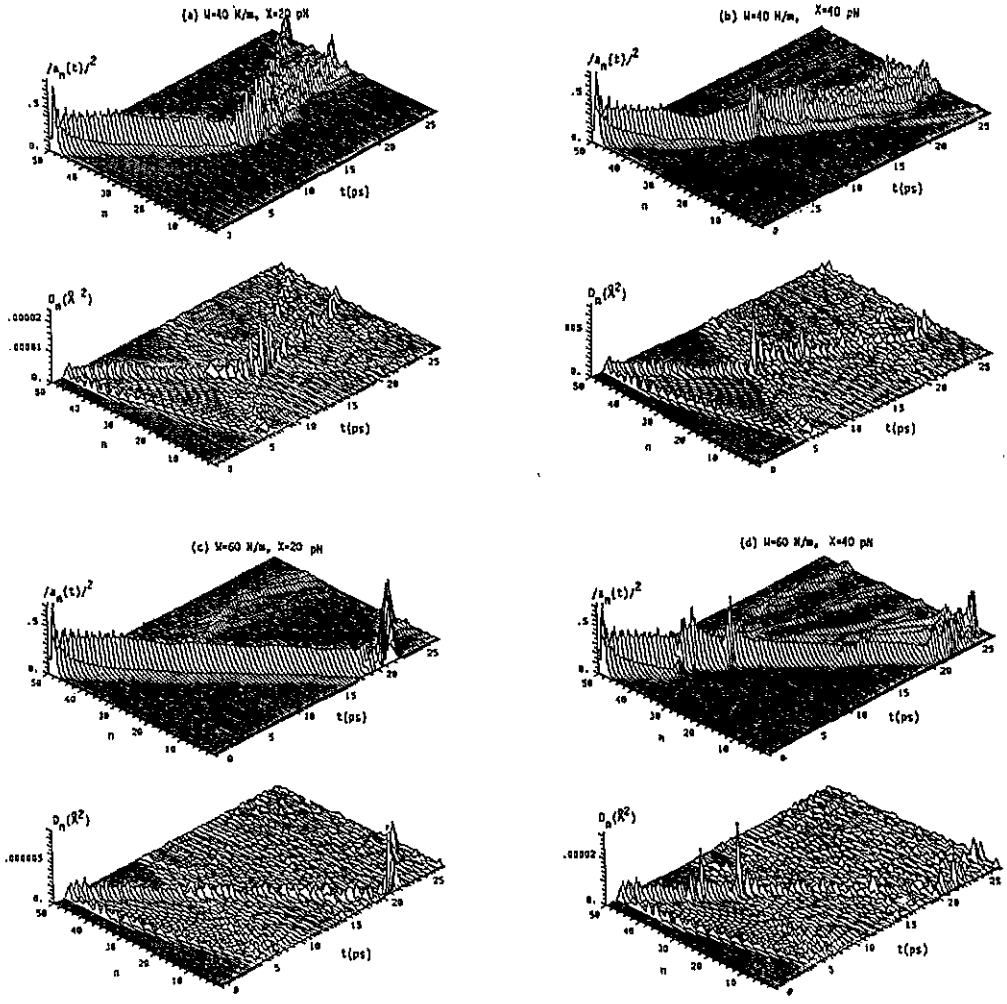

Figure 3. Time evolution of $|a_n(t)|^2$ and of the squared lattice displacements $D_n(t) = [q_{n+1}(t) - q_n(t)]^2$ for four of the parameter sets shown in figure 2: (*a*) $W = 40$ N m^{-1}, $X = 20$ pN; (*b*) $W = 40$ N m^{-1}, $X = 40$ pN; (*c*) $W = 60$ N m^{-1}, $X = 20$ pN; (*d*) $W = 60$ N m^{-1}, $X = 40$ pN.

4. Three-chain simulations at $T = 0$ K

As Scott pointed out (see [25] for a recent review) a long time ago [3], in an α-helix three parallel chains of hydrogen bonds exist, which are coupled by dipole–dipole interactions. If α is an index that specifies the chain ($\alpha = 1$, 2 or 3), and if L is the

coupling parameter between two neighbouring C=O oscillators on different chains, the equations of motion for the simple $|D_2\rangle$ *ansatz* state are [3,24]:

$$i\hbar\dot{a}_{n\alpha} = -J(a_{n+1,\alpha} + a_{n-1,\alpha}) + L(a_{n,\alpha+1} + a_{n,\alpha-1}) + X(q_{n+1,\alpha} - q_{n\alpha})a_{n\alpha} \tag{12}$$

$$M\ddot{q}_{n\alpha} = W(q_{n+1,\alpha} - 2q_{n\alpha} + q_{n-1,\alpha}) + X(|a_{n\alpha}|^2 - |a_{n-1,\alpha}|^2). \tag{13}$$

Scott's argument is now that the usually used values for the parameters W and M apply only for the case of three coupled chains. He found [3] for the interchain coupling parameter a value of $L = 1.54$ meV. For this value of L and standard values for the other parameters ($W = 13$ N m^{-1}, $M = 114m_p$, $X = 62$ pN and $J = 0.967$ meV) we performed simulations for a three-chain system, as Scott did for special cases of excitation [3]. We used the symmetric A mode ($a_{n1} = a_{n2} = a_{n3}$), the linear combination of the two degenerate E modes ($a_{n1} = 0$, $a_{n2} = 1/\sqrt{2}$, $a_{n3} = -1/\sqrt{2}$) and an asymmetric local excitation (L) of one unit on a single chain. The results are shown in figure 4. We see that in the case of the A mode the soliton consists of three identical, parallel-moving localized excitations on all three chains, while in the E mode the soliton moves only on two chains. In the case of the local excitation the soliton is found mainly on one chain, with a small fraction of the excitation transferred to the others. However, we did not observe the phenomenon reported by Scott [3] that solitons on one chain jump to another after some time. Maybe the build-up of a small fraction of the excitation on the other chains in the case of the asymmetric initial condition might lead to a transfer of the whole soliton after longer times. In figure 5 we show only one of the chains for each of these simulations. One recognizes immediately that, despite the different initial excitations, the properties of the solitons are very similar in all three cases. Especially, the time that the solitons need to pass once through the chain is in all cases $\simeq 40$ ps.

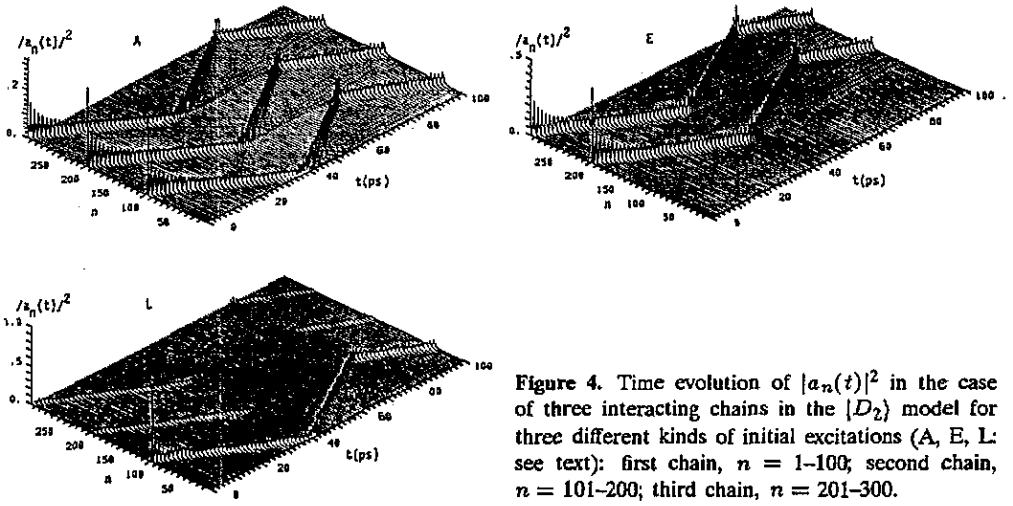

Figure 4. Time evolution of $|a_n(t)|^2$ in the case of three interacting chains in the $|D_2\rangle$ model for three different kinds of initial excitations (A, E, L: see text): first chain, n = 1–100; second chain, n = 101–200; third chain, n = 201–300.

Scott [3,24] argues for the A mode as follows. The norm is given by

$$\sum_{n,\alpha} |a_{n\alpha}|^2 = 1. \tag{14}$$

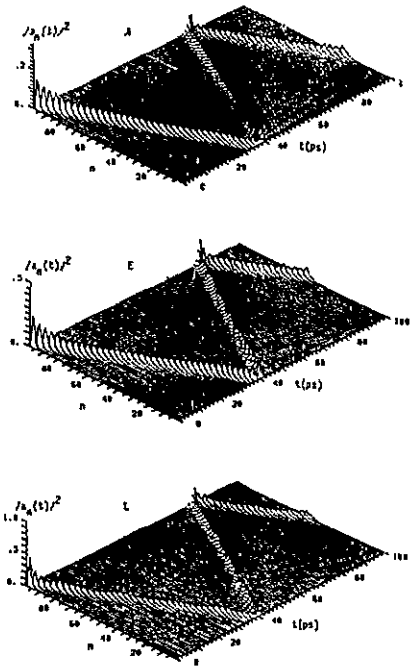

Figure 5. Same as figure 4, but only one chain shown for each simulation: A mode (top), E mode (middle) and L excitation (bottom).

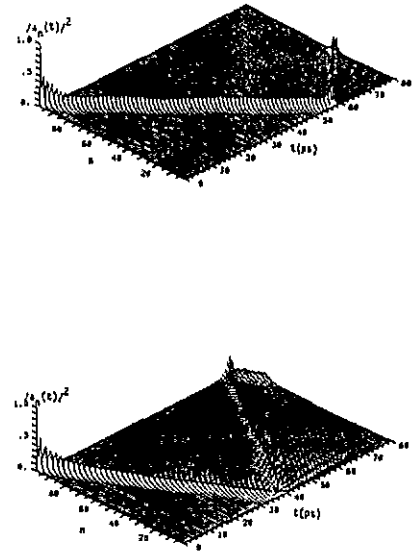

Figure 6. Time evolution of $|a_n(t)|^2$ for isolated chains with $W = 13$ N m^{-1}, $M = 114m_p$ (upper part) and $W = 39$ N m^{-1}, $M = 342m_p$ (lower part) ($|D_2\rangle$ *ansatz*).

If we introduce for the A mode $a_n = (\sqrt{3})a_{n\alpha}$ and $q_n = q_{n\alpha}$ then from the above equation

$$\sum_n |a_n|^2 = 1 \tag{15}$$

holds and we obtain

$$i\hbar\dot{a}_n = -J(a_{n+1} + a_{n-1}) + X(q_{n+1} - q_n)a_n \tag{16}$$

$$3M\ddot{q}_n = 3W(q_{n+1} - 2q_n + q_{n-1}) + X(|a_n|^2 - |a_{n-1}|^2). \tag{17}$$

The term

$$L(a_{n,\alpha+1} + a_{n,\alpha-1}) = (2L/\sqrt{3})a_n \tag{18}$$

was included in the phase transformation on the a_n to obtain these equations of motion. These are identical to the equations for one chain but with $M' = 3M$ and $W' = 3W$. In figure 6 we show simulations of single chains with two combinations of parameters. Obviously one really has to work with $3M$ and $3W$ in order to reproduce the results of three-chain simulations with a one-chain calculation. The important point is that this conclusion holds not only for the symmetric A modes, for which Scott's considerations outlined above are valid, but also for the E mode and even for a single-chain excitation.

In the more complicated $|D_1\rangle$ case the equations of motion for the symmetric A mode are

$$i\hbar\dot{a}_n = a_n \sum_k \{-\tfrac{1}{2}i\hbar(\dot{b}_{nk}b^*_{nk} - \dot{b}^*_{nk}b_{nk}) + \hbar\omega_k[2B_{nk}\,\mathrm{Re}(b_{nk}) + |b_{nk}|^2]\}$$
$$- J(D_{n,n+1}a_{n+1} + D_{n,n-1}a_{n-1}) + 2La_n. \tag{19}$$

As in Scott's derivation for the $|D_2\rangle$ case we dropped the index α for the helix number, because we can set $a_{n\alpha} = a_n/\sqrt{3}$. Since further $D_{n,\alpha,n,\alpha\pm1} = 1$ (because $B_{nk\alpha} = b_{nk,\alpha\pm1}$), the coupling term between neighbouring spines also simplifies and can be taken into the phase transformation on the a_n. Because all coherent state amplitudes for the same site and normal mode on different spines are equal, we have for D_{nm} again:

$$D_{nm} = \exp\left(-\tfrac{1}{2}\sum_k [|b_{nk} - b_{mk}|^2 + 2i\,\mathrm{Im}(b^*_{nk}b_{mk})]\right). \tag{20}$$

In the equations for the coherent state amplitudes the factors at the a_n cancel because the a_n appear only in form of $a_{n\pm1}/a_n$. Further the complicated interchain coupling term vanishes in these equations, because it contains factors $(b_{n,k,\alpha\pm1} - b_{nk\alpha}) = 0$:

$$i\hbar\dot{b}_{nk} = \hbar\omega_k(b_{nk} + B_{nk}) - J[D_{n,n+1}(b_{n+1,k} - b_{nk})a_{n+1}/a_n$$
$$+ D_{n,n-1}(b_{n-1,k} - b_{nk})a_{n-1}/a_n]. \tag{21}$$

The values of ω_k and the matrix **B** are identical for the three lattice systems. Note that the equations shown above are valid only for the symmetric A mode. We see that the equations are completely identical with the equations for one chain, since also here the interchain coupling gives only a phase in the a_n and does not appear explicitly in the calculations. Thus for the A mode no additional computational effort is necessary. The more complicated equations of motion for general excitations are given in section 5. In figure 7 we show the results of three-chain simulations with an A-mode excitation but using the general equations of motion for three chains given in the next section. Further we show again the two single-chain simulations, but now computed in the $|D_1\rangle$ model ($X = 62$ pN, figure 7(*a*)). In addition we have also used the large value of $X = 180$ pN (figure 7(*b*)) because, as previous results [17,19] have shown, in the $|D_1\rangle$ model at $T = 0$ K solitons appear only for very large values of the exciton–phonon coupling constant. We see from figure 7(*a*) that the one-chain results for parameters M and W are the same as those from the explicit three-chain calculations as expected from the considerations outlined above. For $X = 180$ pN (figure 7(*b*)) we observe a travelling solitary wave in the three-chain simulation as expected from the one-chain results. However, an A-mode excitation does not necessarily occur in reality and thus we also have to study initial excitations in the E mode and ones that are localized on one chain where the equations for one chain are not the same as those for three interacting chains. This is discussed in the next section.

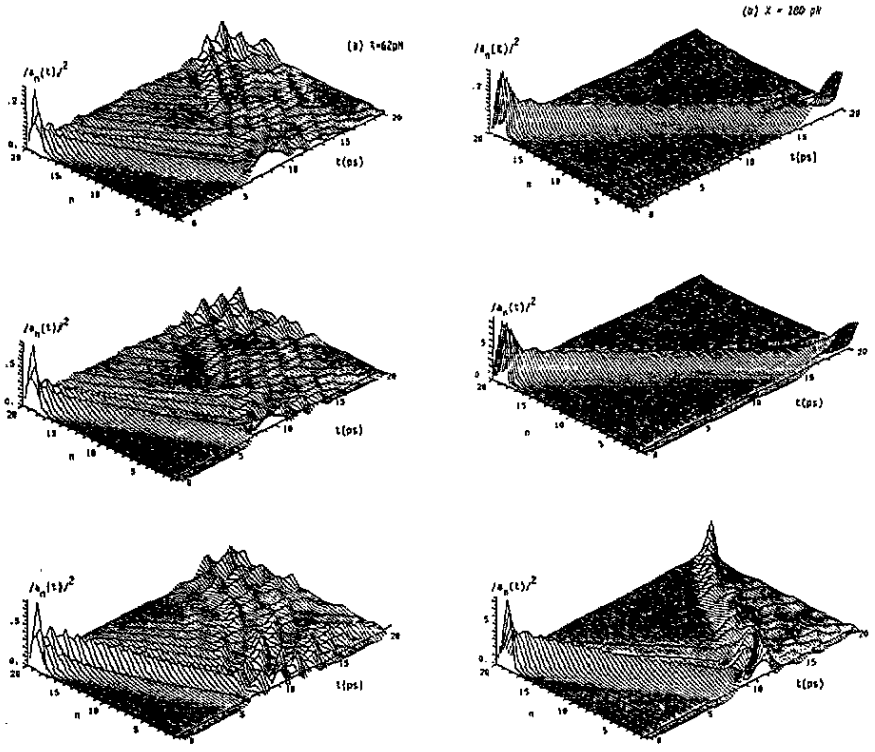

Figure 7. *Time evolution of* $|a_n(t)|^2$ ($|D_1\rangle$ *ansatz state) for three interacting chains* with an A-mode excitation (only one chain shown: upper part) and for isolated chains with $W = 13$ N m^{-1}, $M = 114m_p$ (middle) and $W = 39$ N m^{-1}, $M = 342m_p$ (lower part), for (*a*) $X = 62$ pN and (*b*) $X = 180$ pN.

5. Three-chain dynamics at $T = 300$ K

Here we want to show first the necessary equations for three-chain dynamics with general initial excitations in the $|D_1\rangle$ case using Davydov's model for temperature effects. The *ansatz* state is the usual one, where n runs over the N sites of a spine, α over the three spines and k over the $(N-1)$ normal modes of the decoupled spines (the translational mode has to be excluded from the summation):

$$|D_1, \nu\rangle = \sum_{n,\alpha} a_{n\alpha}(t)\hat{a}^+_{n\alpha}|0\rangle_e \exp\left(\sum_{k=1}^{N-1}[b_{nk\alpha}(t)\hat{b}^+_{k\alpha} - b^*_{nk\alpha}(t)\hat{b}_{k\alpha}]\right)|\nu\rangle. \tag{22}$$

The overlaps between the coherent states are now

$$D_{n\alpha m\beta} = \exp\left(\sum_{k=1}^{N-1}[(v_k+1)b^*_{nk\alpha}b_{mk\beta} + v_k b_{nk\alpha}b^*_{mk\beta} - (v_k+\tfrac{1}{2})(|b_{nk\alpha}|^2 + |b_{mk\beta}|^2)]\right). \tag{23}$$

To simplify notation, we define

$$D_{n,n\pm1,\alpha} \equiv D_{n,\alpha,n\pm1,\alpha} \qquad D_{n,\alpha,\alpha\pm1} \equiv D_{n,\alpha,n,\alpha\pm1}. \tag{24}$$

Note that in our notation α has to be taken modulo 3 since for the interaction between the three spines we have cyclic boundary conditions (not for the interactions within one spine). The thermally averaged Hamiltonian is now

$$H_T = \sum_{n,\alpha}\Big(E_0|a_{n\alpha}|^2 - J(a^*_{n\alpha}a_{n,n+1,\alpha}D_{n,n+1,\alpha} + a^*_{n\alpha}a_{n-1,\alpha}D_{n,n-1,\alpha}) + L(a^*_{n\alpha}a_{n,\alpha+1}D_{n,\alpha,\alpha+1} + a^*_{n\alpha}a_{n,\alpha-1}D_{n,\alpha,\alpha-1}) + |a_{n\alpha}|^2\sum_{k=1}^{N-1}\hbar\omega_k[B_{nk}(b_{nk\alpha}+b^*_{nk\alpha}) + v_k + \tfrac{1}{2} + |b_{nk\alpha}|^2]\Big). \tag{25}$$

The equations of motion are obtained with the Euler–Lagrange method. After the phase transformation

$$a_{n\alpha}(t) = a'_{n\alpha}(t)\exp\left[-\frac{\mathrm{i}}{\hbar}\Big(E_0 + \sum_{k=1}^{N-1}\hbar\omega_k(v_k+\tfrac{1}{2})\Big)t\right] \tag{26}$$

and renaming $a'_{n\alpha}$ as $a_{n\alpha}$ again, they read as

$$\mathrm{i}\hbar\dot{a}_{n\alpha} = a_{n\alpha}\sum_{k=1}^{N-1}\Big(-\frac{\mathrm{i}\hbar}{2}(\dot{b}_{nk\alpha}b^*_{nk\alpha} - \dot{b}^*_{nk\alpha}b_{nk\alpha}) + \hbar\omega_k[B_{nk}(b_{nk\alpha}+b^*_{nk\alpha}) + |b_{nk\alpha}|^2]\Big) - J(D_{n,n+1,\alpha}a_{n+1,\alpha} + D_{n,n-1,\alpha}a_{n-1,\alpha}) + L(D_{n,\alpha,\alpha+1}a_{n,\alpha+1} + D_{n,\alpha,\alpha-1}a_{n,\alpha-1}) \tag{27}$$

and

$$\begin{aligned}\mathrm{i}\hbar\dot{b}_{nk\alpha} = {}& \hbar\omega_k(B_{nk} + b_{nk\alpha}) - J\{(b_{n+1,k,\alpha} - b_{nk\alpha})\\ &\times[(v_k+1)D_{n,n+1,\alpha}(a_{n+1,\alpha}/a_{n\alpha}) + v_kD_{n+1,n,\alpha}(a^*_{n+1,\alpha}/a^*_{n\alpha})]\\ &+ (b_{n-1,k,\alpha} - b_{nk\alpha})[(v_k+1)D_{n,n-1,\alpha}(a_{n-1,\alpha}/a_{n\alpha}) + v_kD_{n-1,n,\alpha}\\ &\times(a^*_{n-1,\alpha}/a^*_{n\alpha})]\} + L\{(b_{n,k,\alpha+1} - b_{nk\alpha})[(v_k+1)D_{n,\alpha,\alpha+1}\\ &\times(a_{n,\alpha+1}/a_{n\alpha}) + v_kD_{n,\alpha+1,\alpha}(a^*_{n,\alpha+1}/a^*_{n\alpha})]\\ &+ (b_{n,k,\alpha-1} - b_{nk\alpha})[(v_k+1)D_{n,\alpha,\alpha-1}(a_{n,\alpha-1}/a_{n\alpha})\\ &+ v_kD_{n,\alpha-1,\alpha}(a^*_{n,\alpha-1}/a^*_{n\alpha})]\}.\end{aligned} \tag{28}$$

Let us first discuss a localized excitation at one of the terminal sites of just one spine. We have chosen a chain length of 20 units for each chain (excitation at site 19 of chain 1) and the usual value of 1.5373 meV for the interchain coupling L [25]. The time step was chosen as 0.25 fs. In this case in a typical calculation on localized initial excitations the total energy was conserved within roughly 2 μeV and the norm to better than 5 ppb (parts per billion). Repetition of one of the calculations with a time step of 0.1 fs led to no changes in the results.

In figure 8 we show the results of these simulations. We use for W the values 13 N m^{-1} from measurements on formamide crystals and 19 N m^{-1} from theoretical calculations. For X we use 35 N m^{-1}, which was found by Scott, and also the usually applied value of 62 pN (see [25] for references). Figures 8(a) and (b) show that for $W = 13$ N m^{-1} in the case of the lower X value a solitary wave is formed first, which becomes trapped roughly in the middle of the chain, while for the larger X value the excitation is trapped close to the chain end. In both cases a considerable part of the excitation goes over to the initially unexcited chains. In the case of $W = 19$ N m^{-1} (figures 8(c) and (d)) at the lower X value a clear solitary wave is formed and travels through the chain. If one looks more closely at the pulse-like structure, one sees that the excitation is oscillating between the initially excited chain and the other two. When the excitation probability is small on chain 1, it is large on chains 2 and 3 and vice versa. At the larger X value the excitation is again trapped close to the initial excitation site. For $X = 62$ pN we have increased W to 30, 40, 50 and 60 N m^{-1}. Two cases are shown in figures 8(e) (40 N m^{-1}) and (f) (60 N m^{-1}). As in the case of one-chain simulations an increase in W favours soliton formation and we found solitons occurring between $W = 40$ and 60 N m^{-1}, even quantitatively in fair agreement with one-chain and even with $|D_2\rangle$ results.

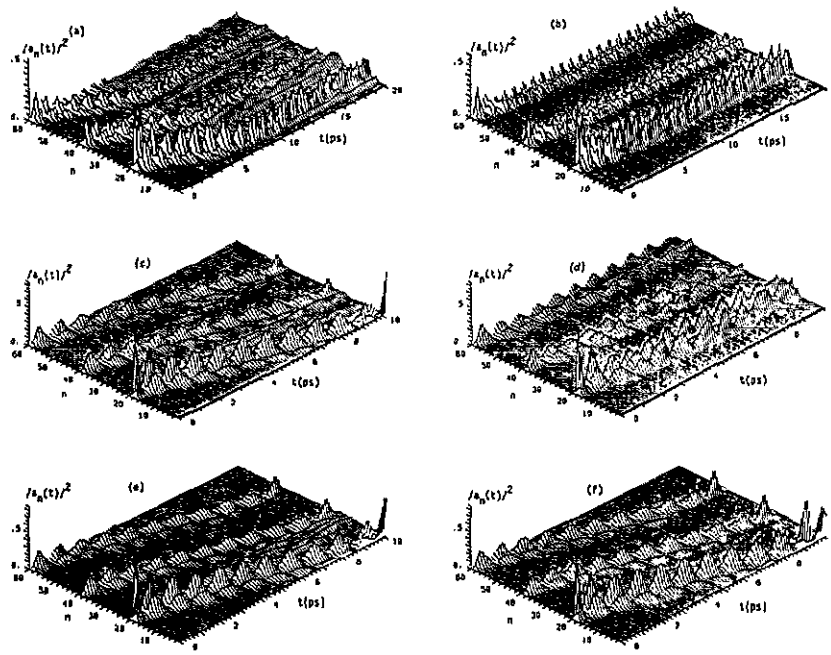

Figure 8. Time evolution of $|a_n(t)|^2$ in the $|D_1\rangle$ *ansatz* state at 300 K using Davydov's model for temperature effects and a localized initial excitation ($a_{19,1}(0) = 1$, all other a equal to 0.005, then normalized to 1). All three chains are shown: chain 1, n = 1–20; chain 2, n = 21–40; chain 3, n = 41–60. Time step, 0.25 fs. For different values of W and X: (a) $W = 13$ N m^{-1}, $X = 35$ pN; (b) $W = 13$ N m^{-1}, $X = 62$ pN; (c) $W = 19$ N m^{-1}, $X = 35$ pN; (d) $W = 19$ N m^{-1}, $X = 62$ pN; (e) $W = 40$ N m^{-1}, $X = 62$ pN; (f) $W = 60$ N m^{-1}, $X = 62$ pN.

As figure 9 shows, the results for the E mode are more or less similar. However, here the solitary waves formed usually do not survive the reflection at the chain end. But we know from the one-chain results that this should be a pure end effect and

that the solitary waves should be able to pass also through considerably longer chains [20]. What we observe further is that a considerable part of the excitation remains localized at the initial excitation site. Figures 9(*e*) and (*f*) for larger W values again indicate that from $W = 40$ N m^{-1} solitary wave formation can be expected. In figure 10 we show the results for the symmetric A mode. Here we show only one of the three chains, because the results for the other two are identical. It is obvious that a strong tendency to trapping after a few sites shows up. However, for $W = 19$ N m^{-1} and $X = 35$ pN again a solitary wave is formed. In the cases of larger W values we observe again solitary wave formation, but at 40 N m^{-1} (figure 10(*e*)) after the reflection the soliton oscillates around the chain end. At $W = 50$ N m^{-1} (figure 10(*f*)) the soliton survives the reflection but a part of the excitation becomes trapped. Increasing W to 60 N m^{-1} (not shown here) leads again to a solitary wave, but it moves erratically after reflection. Thus we reach the same basic conclusion as in the case of most other models (with the exception of the partial dressing state [26]) that we studied [23]: if W is larger than 30–40 N m^{-1} solitary wave formation should be possible in proteins also at physiological temperature.

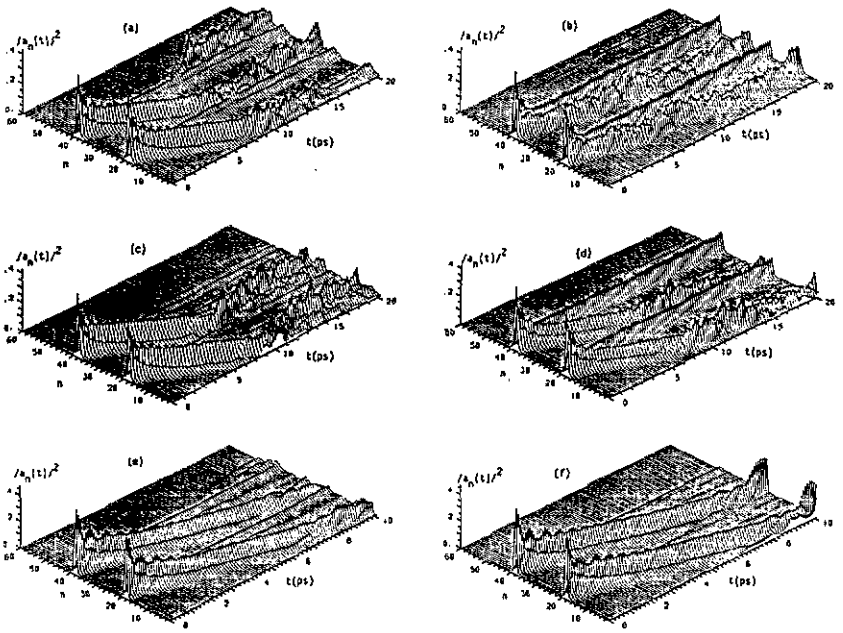

Figure 9. Same as figure 8 but for an E-mode initial excitation at sites 19 of two of the chains ($a_{19,1}(0) = -a_{19,2}(0) = 1/\sqrt{2}$, all other a equal to 0.005, then normalized to 1). For: (*a*) $W = 13$ N m^{-1}, $X = 35$ pN; (*b*) $W = 13$ N m^{-1}, $X = 62$ pN; (*c*) $W = 19$ N m^{-1}, $X = 35$ pN; (*d*) $W = 19$ N m^{-1}, $X = 62$ pN; (*e*) $W = 30$ N m^{-1}, $X = 62$ pN; (*f*) $W = 40$ N m^{-1}, $X = 62$ pN.

6. Conclusions

For the $|D_2\rangle$ *ansatz* state we performed soliton dynamics in a system of three coupled chains as suggested and done earlier by Scott *et al* [3]. We could verify Scott's proposal

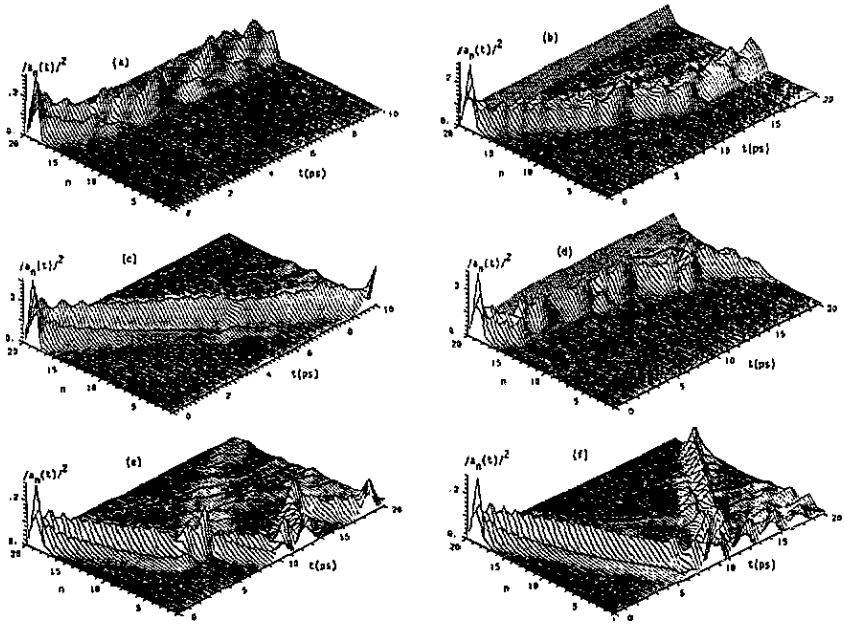

Figure 10. Same as figure 8, but for an initial symmetric A-mode excitation ($a_{19,1}(0) = a_{19,2}(0) = a_{19,3}(0) = 1/\sqrt{3}$, all other a equal to 0.005, then normalized to 1). Here only one of the chains is shown, because the results for all chains are identical. For: (*a*) $W = 13$ N m^{-1}, $X = 35$ pN; (*b*) $W = 13$ N m^{-1}, $X = 62$ pN; (*c*) $W = 19$ N m^{-1}, $X = 35$ pN; (*d*) $W = 19$ N m^{-1}, $X = 62$ pN; (*e*) $W = 40$ N m^{-1}, $X = 62$ pN; (*f*) $W = 50$ N m^{-1}, $X = 62$ pN.

that three-chain dynamics can be simulated with one-chain calculations if one takes as site mass three times the value applied in the three-chain dynamics and for the spring constant of the hydrogen bonds also three times the value for one bond. This result is independent of the initial excitation, which can correspond to the symmetric A mode or to the degenerate E mode of the three-chain system. Even for a localized excitation on one chain we obtained agreement between three-chain dynamics and those using one chain but changed parameters.

For the $|D_1\rangle$ state we surveyed again the (X, W) parameter space at 300 K using one chain and $3M$ as site mass within Davydov's method. We found that W has to be larger than roughly 70 N m^{-1} to allow soliton formation around $X = 60$ pN. Since, according to Scott's reasoning based on the $|D_2\rangle$ *ansatz*, this value would correspond to a spring constant of about 25 N m^{-1}, we arrive more or less at the same conclusion as discussed above for one chain with a smaller mass, if the suggestion that three-chain dynamics could be reproduced by one-chain simulations with a site mass of $3M$ is correct also in the $|D_1\rangle$ case. However, at 0 K we found that in the $|D_1\rangle$ case three-chain dynamics with parameters M, W and X are identical to one-chain simulations with the same parameters in contrast to $|D_2\rangle$ dynamics.

With explicit three-chain simulations at $T = 300$ K using Davydov's temperature model we found again that solitary waves are formed at W values larger than 30–40 N m^{-1}. However, if X is around 35 pN instead of 62 pN already from W around 19 N m^{-1} solitary waves were observed. Thus the conclusion drawn earlier by us remains unchanged: if the spring constant of the hydrogen bonds in

protein α-helices is larger than 30–40 N m^{-1} the Davydov soliton should be able to function at 300 K. Interestingly this conclusion is reached with both of Davydov's *ansatz* states and with different models for temperature effects. Since the usually quoted value of 13 N m^{-1} derives from formamide crystals where the hydrogen-bonded molecules vibrate freely, it should be too small for proteins. In proteins the hydrogen-bonded sites are embedded in the covalent backbone of the helix, which becomes distorted due to the vibration. Thus we expect the spring constant of a protein normal mode corresponding to hydrogen-bond stretch to be much larger than that of crystalline formamide, and thus probably allowing for Davydov solitons to be formed in proteins. However, calculations or measurements on the spring constant in proteins are necessary to decide finally on the question of the existence of Davydov solitons.

Acknowledgments

First of all it is a pleasure to thank Professor A C Scott for fruitful discussions and correspondence on the topic of this work. Further the financial support of the 'Deutsche Forschungsgemeinschaft' (Project Ot 51/6-2) and the 'Fond der Chemischen Industrie' is gratefully acknowledged.

References

[1] Davydov A S and Kislukha N I 1973 *Phys. Status Solidi* b **59** 465
Davydov A S 1979 *Phys. Scr.* **20** 387
[2] Davydov A S 1980 *Zh. Eksp. Teor. Fiz.* **78** 789 (Engl. Transl. 1980 *Sov. Phys.-JETP* **51** 397)
[3] Scott A C 1982 *Phys. Rev.* A **26** 57; 1984 *Phys. Scr.* **29** 279
MacNeil L and Scott A C 1984 *Phys. Scr.* **29** 284; 1985 *Phil. Trans. R. Soc.* A **315** 423
[4] Förner W and Ladik J 1991 *Davydov's Soliton Revisited* ed P L Christiansen and A C Scott, NATO ASI, Ser. B, Physics, vol 243 (New York: Plenum) p 267
[5] Halding J and Lomdahl P S 1987 *Phys. Lett.* **124A** 37
[6] Lomdahl P S and Kerr W C 1985 *Phys. Rev. Lett.* **55** 1235; 1991 *Davydov's Soliton Revisited* ed P L Christiansen and A C Scott, NATO ASI, Ser. B, Physics, vol 243 (New York: Plenum)
[7] Kerr W C and Lomdahl P S 1987 *Phys. Rev.* B **35** 3629
[8] Kerr W C and Lomdahl P S 1991 *Davydov's Soliton Revisited* ed P L Christiansen and A C Scott, NATO ASI, Ser. B, Physics, vol 243 (New York: Plenum)
[9] Lawrence A F, McDaniel J C, Chang D B, Pierce B M and Birge R R 1986 *Phys. Rev.* A **33** 1188
[10] Bolterauer H 1986 *Structure Coherence and Chaos* Proc. MIDIT 1986 Workshop (Manchester: Manchester University Press); 1991 *Davydov's Soliton Revisited* ed P L Christiansen and A C Scott, NATO ASI, Ser. B, Physics, vol 243 (New York: Plenum)
[11] Cottingham J P and Schweitzer J W 1989 *Phys. Rev. Lett.* **62** 1792
Schweitzer J W and Cottingham J P 1991 *Davydov's Soliton Revisited* ed P L Christiansen and A C Scott, NATO ASI, Ser. B, Physics, vol 243 (New York: Plenum)
[12] Motschmann H, Förner W and Ladik J 1989 *J. Phys.: Condens. Matter* **1** 5083
[13] Förner W 1991 *J. Phys.: Condens. Matter* **3** 4333
[14] Förner W 1992 *J. Comput. Chem.* **13** 275
[15] Brown D W, Lindenberg K and West B J 1986 *Phys. Rev.* A **33** 4104, 4110; 1987 *Phys. Rev.* B **35** 6169; 1988 *Phys. Rev.* B **37** 2946
Brown D W 1988 *Phys. Rev.* A **37** 5010
[16] Cruzeiro L, Halding J, Christiansen P L, Skovgaard O and Scott A C 1988 *Phys. Rev.* A **37** 880
[17] Mechtly B and Shaw P B 1988 *Phys. Rev.* B **38** 3075
[18] Skrinjar M J, Kapor D V and Stojanovic S D 1988 *Phys. Rev.* A **38** 6402
[19] Förner W 1991 *Phys. Rev.* A **44** 2694; 1993 *Nonlinearity with Disorder* ed St Pnevmatikos, F Kh Abdullaev and A R Bishop (Heidelberg: Springer) to appear

[20] Förner W 1992 *J. Phys.: Condens. Matter* **4** 1915
[21] Förner W 1993 *Nanobiology* at press
[22] Wang X, Brown D W and Lindenberg K 1989 *Phys. Rev. Lett.* **62** 1796
[23] Förner W 1993 *J. Phys.: Condens. Matter* **5** 803
[24] Scott A C 1990 presented at *Conf. on Nonlinear Sciences: The Next Decade* Los Alamos National Laboratory, 21 May 1990
[25] Scott A C 1993 *Phys. Rep.* at press
[26] Brown D W and Ivic Z 1989 *Phys. Rev.* B **40** 9876